Proceedings World Geothermal Congress 2020+1
Reykjavik, Iceland, April - October 2021

Review of Aeromagnetic Data Processing in Geothermal Gradient Estimation in Mexico

Juan L. Carrillo-de la Cruz[1]*, Rosa M. Prol-Ledesma[2] and Dario Gómez-Rodríguez[3]

[1]Posgrado en Ciencias de la Tierra. Institute of Geophysics, Universidad Nacional Autónoma de México, Cd. Universitaria, México D.F., 04510, México

[2]Institute of Geophysics, Universidad Nacional Autónoma de México, Cd. Universitaria, México D.F., 04510, México

División Académica de Ciencias Básicas, Universidad Juárez Autónoma de Tabasco, Cunduacán, Tabasco, 86690, México.

*juanluiscc9@comunidad.unam.mx

Keywords: Curie Temperature Depth, Depth to the Bottom of Magnetic Sources, Geothermal Gradient, Aeromagnetic Data.

ABSTRACT

Estimation of the geothermal gradient using the depth of the magnetic source base is widely used in diverse geological environments. However, the determination of the base of the magnetic source does not necessarily represent the Curie Temperature depth, especially in complex geological provinces, as is the case of Mexico. Geothermal gradient has been determined in numerous sites that can be compared with the aeromagnetic data processing results. The occurrence of large differences has been documented. In this work, we present the coincidences and inconsistencies of the method, and the parameters that affect the geothermal gradient estimation.

1. INTRODUCTION

The study of the thermal structure of the earth using direct temperature measurements is complex because obtaining thermal data from wells is expensive and slow. For this reason, is common to use alternative temperature estimators at depth, such as silica geothermometers or the Curie temperature depth (CTD). The CTD is calculated by spectral analysis of aeromagnetic data, obtained in an aircraft or satellite, using different methodologies to determine the bottom of the magnetic source. The depth to the bottom of the magnetic source is assumed to be linked to the Curie temperature; therefore, this depth determines the conductive geothermal gradient and heat flow may be estimated using that value (Okubo et al., 1985; Haggerty, 1978; Gasparini et al., 1979; Conrad et al., 1983; Blakely, 1988; Campos-Enriquez et al., 1980; Wasilewski and Mayhew, 1992; Tsokas et al., 1998; Tanaka et al., 1999; Ross et al., 2006; Espinosa-Cardeña and Campos-Enriquez, 2008; Bouligand et al., 2009; Li et al., 2010; Manea and Manea, 2011; Hsieg et al., 2014; Rosales et al., 2014; Gao et al., 2015; Li et al., 2017; Martos et al., 2017; Martos et al., 2018).

Before the spectral analysis is performed, pre-processing of the aeromagnetic data considers the regional geology and window size, these operations will add spurious effects in the results that will be carry over or sub estimations. These effects will result in a thermal model that is not representative of the study area. In this work, we analyze results from published calculations of the depth to the bottom of the magnetic source, and recalculate the data using a fractal model of the magnetization to identify the effect in the results of the diverse processing techniques.

2. DATA AND METHODS

The data processing technique is critical for the results of the depth to the bottom of magnetic source (DBMS). For this reason, and following the recommendation proposed by Ravat et al. (2007), before the spectral analysis is implemented, the following recommendations must be considered:

- Analysis windows must have a side length up to 10 times the expected bottom depth; nevertheless, Salem et al. (2014) considered a window side length up to 6 times the expected DBMS to reach the deepest magnetic layers.
- Arbitrary filtering must be avoided to remove regional fields and compiling magnetic anomalies derived from International Geomagnetic Reference Field (IGRF) with spherical harmonic of degree 13 or Comprehensive Models, because arbitrary filtering affects the low wavenumbers.
- Apply the Shuey et al. (1977) autocorrelation function and validate the calculated DBMS only in windows where the autocorrelation function presents circularity, that is, with no strong data trends.
- Repeat calculations with different window size, starting with large windows and reducing the size to improve spatial resolution.

In addition to the Ravat et al. (2007) considerations, we recommend the use of the magnetization fractal approach and be cautious with high fractal exponents, because an overcorrected spectrum yields shallower estimations than actual DBMS.

2.1 Data

The data used in this study were compiled from the North America Magnetic Anomaly Group (Fig. 1) as part of the collaboration between the Consejo de Recursos Minerales (now Mexican Geological Survey), Geological Survey of Canada and the United States Geological Survey. The data from Mexico were acquire from 1962 to 1992 and digitalized manually, subtracting the Definitive Geomagnetic Reference Field (DGRF), minimum curvature grid, and filtered by the first vertical derivative in poorly merged areas. From 1994 to 2002, the acquisition was done with Cesium magnetometers positioned by differential GPS along north-south-trending

flight lines spaced 1,000 m, flight height from 300 to 400 m above the terrain, and data corrections by diurnal variations of the magnetic field, lag heading, DGRF/IGRF and tie-line mis-ties (NAMAG, 2002).

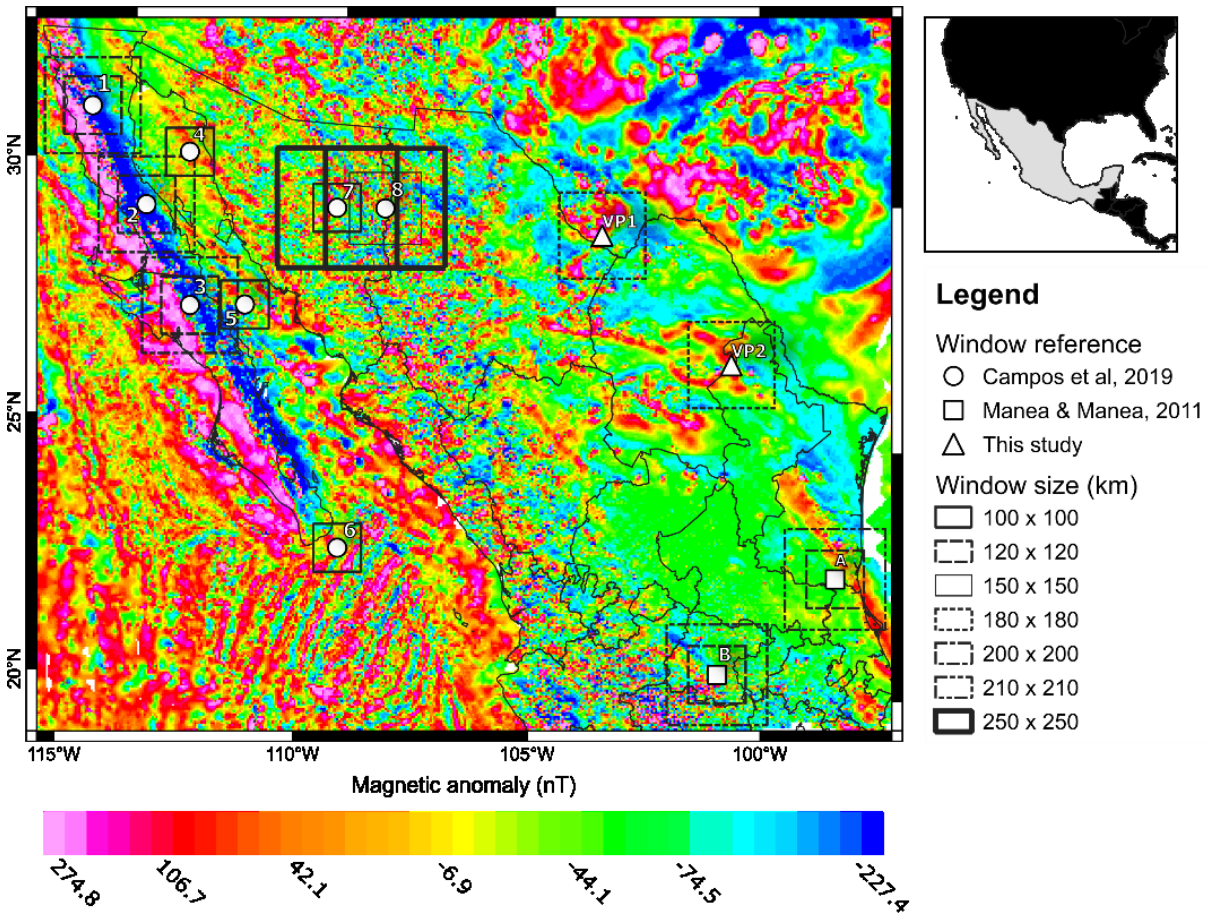

Figure 1: NAMAG data. The window numbers indicate the reference of results in Table 1.

In the North America Anomaly Map, the data grid had 1-km spacing, used the Spherical Transverse Mercator projection, and had a central meridian of 100° W, a base latitude of 0°, a scale factor of 0.926 and an Earth radius of 6,371,204 m (DNAG projection). The values correspond to the magnetic field at 305 m height. Ravat et al. (2007), Bouligand et al. (2009), Manea and Manea (2010), Espinoza-Cardeña et al. (2016) and Campos-Enríquez et al. (2019) used NAMAG data in spectral analysis studies and DBMS estimations.

2.2 Methods

DBMS was calculated using the methodology developed by Salem et al. (2014), which emphasizes the fractal behavior of magnetization as a power-law correction of the spectra and the forward modelling of the spectral peak using the estimations of the centroid method (Pilkington and Todoeschuck, 1993; Maus and Dimri, 1995; Bouligand et al. 2009). The radially averaged power density spectrum, assuming a layer that extends infinitely in all horizontal directions as a random and uncorrelated function of the magnetization (Blakely, 1995, Tanaka et al., 1999) is defined as:

$$P(k) = Ae^{-2kZ_t}\left(1 - e^{-k(Z_b - Z_t)}\right)^2 \quad (1)$$

where A is a constant related with the directional factor of the magnetization and the directional factor of the geomagnetic field, Z_t is the depth to the top of the magnetic sources, and Z_b is the DBMS and k is the radial wave number. For wavelengths less than about twice the layer thickness and a signal where the top of magnetic sources dominates the power spectrum (Spector and Grant, 1970; Bhattacharyya and Leu, 1975; Okubo et al., 1985; Tanaka et al., 1999), eq (1) is written as:

$$\ln[P(k)] = \ln A - 2kZ_t \, . \quad (2)$$

Tanaka et al. (1999) propose a different form of eq. (2) in terms of the centroid of the magnetic source (Z_0):

$$P(k) = Be^{-2kZ_0}\left(e^{-k(Z_t - Z_0)} - e^{-k(Z_b - Z_0)}\right)^2 \quad . \quad (3)$$

Following Bhattacharyya and Leu (1975), Okubo et al. (1985) and Tanaka et al. (1999), the simplification of the eq. (3) is used to compute Z_0:

$$\ln[P(k)/k^2] = \ln B - 2kZ_0 \ . \tag{4}$$

The estimation of Z_t and Z_0 is done computing the slope of a straight-line in the high- and low-wavenumbers, respectively. There are uncertainties associated with the straight-line fit that are calculated by the method proposed by Okubo and Matsunaga (1994), using:

$$\epsilon = \frac{\sigma_r}{k_2 - k_1} \tag{5}$$

where ϵ is the uncertainty, σ_r is the standard deviation between the radial power spectrum and the straight-line derived by the linear fit, $k_2 - k_1$ is the wavenumber range used to calculate the straight-line. This uncertainty is always less than 15%. For the calculation of the DBMS (Z_b) we used the Okubo et al. (1988) approach:

$$Z_b = 2Z_0 - Z_t \ . \tag{6}$$

The uncertainty is calculated (Martos et al., 2017) using:

$$\Delta Z_b = \sqrt{4\Delta Z_0^{\,2} + \Delta Z_t^{\,2}} \tag{7}$$

where ΔZ_0 and ΔZ_t are the uncertainties of the depths to the centroid and the top of the magnetic source. The De-fractal approach is based on the fractal distribution of the magnetic source, expressed by:

$$P_R(k) = P_F(k)k^{\alpha} \tag{8}$$

where $P_F(k)$ is the observed power spectrum, $P_R(k)$ is the power spectrum due to a random magnetization model, and α is the fractal parameter related to β by $\alpha = \beta - 1$ (Salem et al., 2014). Correcting the observed power spectrum, it is possible to calculate the DBMS following the flowchart presented in Fig. 2. Evaluation of Z_t, Z_b and α requires the visual inspection and calculation of the misfit between $P_F(k)$ and $P_R(k)$. The misfit R is calculated using the equation:

$$R = \sqrt{\frac{1}{n}\sum_{i=1}^{n}\left(P_R(k) - P_{syn}(k)\right)^2} \ . \tag{9}$$

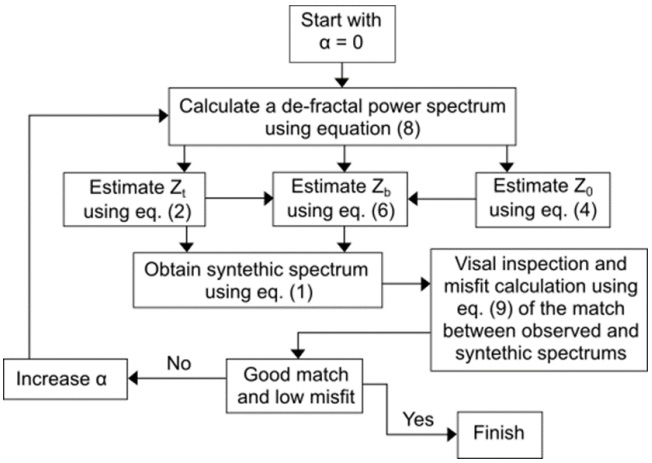

Figure 2: De-fractal method flowchart for the application of the method.

3. CALCULATION OF THE DEPTH TO THE BOTTOM OF THE MAGNETIC SOURCE IN MEXICO

The calculations were carried out in 8 locations from Campos-Enriquez et al. (2019), 2 locations from Manea and Manea (2011) and 2 locations analyzed for this study. The window centers are in the states of Baja California, Baja California Sur, Chihuahua, Coahuila, Guanajuato, Sonora, San Luis Potosí, Tamaulipas and Veracruz (Fig. 1).

We calculated the power spectrum using the Fast Fourier Transform (FFT). As pre-processing, the first-order trend was removed and, to make the edges continuous, grids were expanded 10% using the maximum entropy method on variable window size according to previous DBMS studies; window size varied from 100 x 100 km to 250 x 250 km. For every window, the autocorrelation function was calculated in order to analyze the near circularity and to detect possible trends in the data. According to the flowchart (Fig. 1), the calculation of Z_b, Z_t, and α are done by trial and error to achieve the best match between the observed spectrum and the spectrum due to a random magnetization model (Fig. 3).

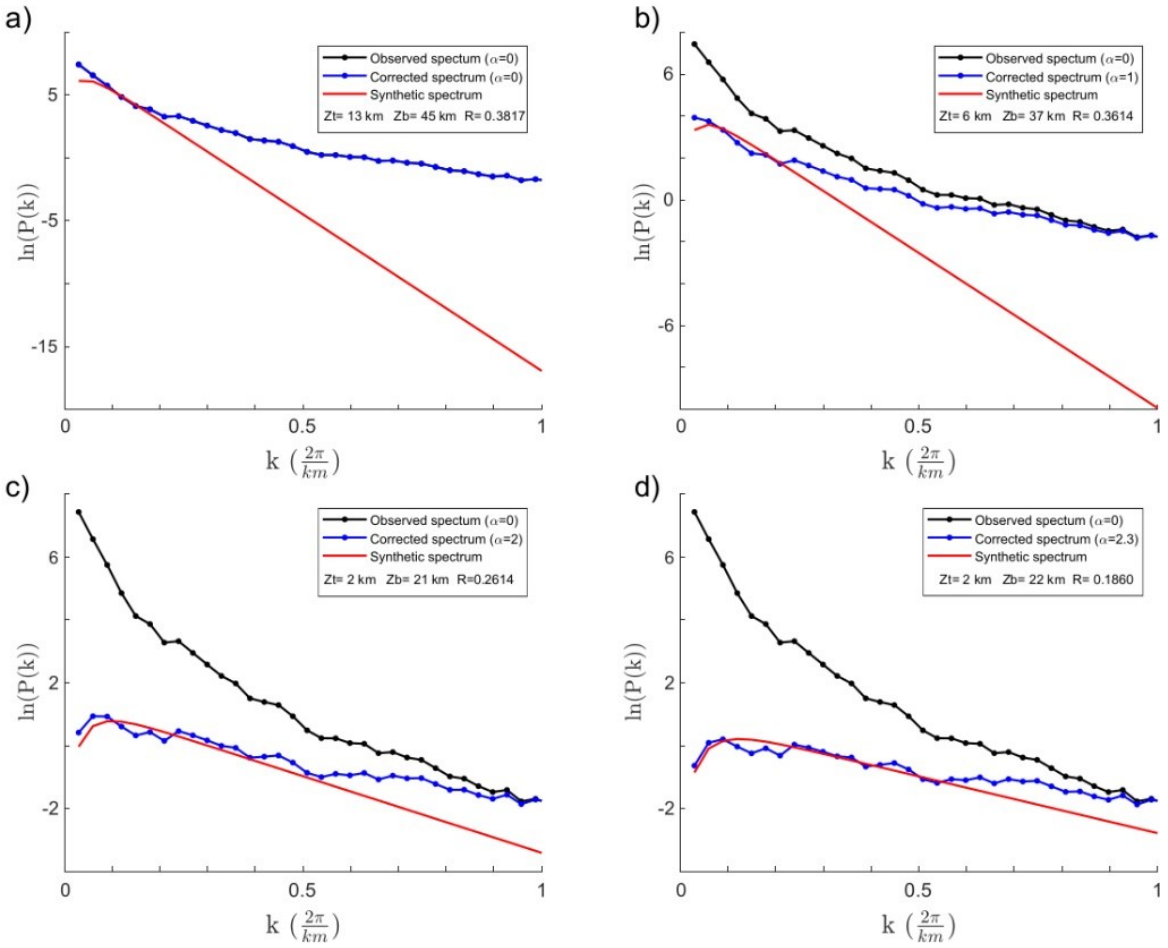

Figure 3: DBMS calculation for window VP1. a) α=0, b) α=1, c) α=2 and d) α=2.3. These figures show the visual change and the misfit obtained for different values of α. Visual inspection and low values of R indicate a good fit.

Forward modeling adjustment is better, with low misfit values, where the autocorrelation function is near-circular. When magnetic data has strong trends, the autocorrelation function is ellipsoidal and presents higher misfit values. The DBMS calculation could be erroneous because the strong trends modify the slopes in the spectra (Shuey et al., 1977); therefore, the synthetic spectrum does not match the corrected spectrum (Fig 4).

4. RESULTS

Calculated DBMS in 19 windows are related with the tectonostratigraphic terranes; some windows yield poor results because the center of the window is located on the boundary of two terranes and the signal could be contaminated by diverse magnetic sources (Ross et al., 2006; Bouligand et al., 2009). Table 1 shows the results obtained from this study. The main issues related with the autocorrelation function or the fit of the power spectrum are mentioned in the observations.

There are differences between the calculation with different window size in window 7, where the DBMS is 9.9 km in the 100 x 100 km window and 18.5 km in the 250 x 250 km window. In both windows the autocorrelation function is near to circular, nevertheless, Campos-Enriquez et al. (2019) mentioned that smaller windows do not provide information of deep crustal magnetic sources because the slope is not well defined. This phenomenon is presented in our estimations because the spectral peak of the corrected spectrum is not well defined. In this study, for the windows 1, 2, 3 and 6 in the Baja California Peninsula, the autocorrelation function presents a strong trend caused probably by the batholithic rocks that have the same tendency. Window A has problems related to the lack of data inside of the window.

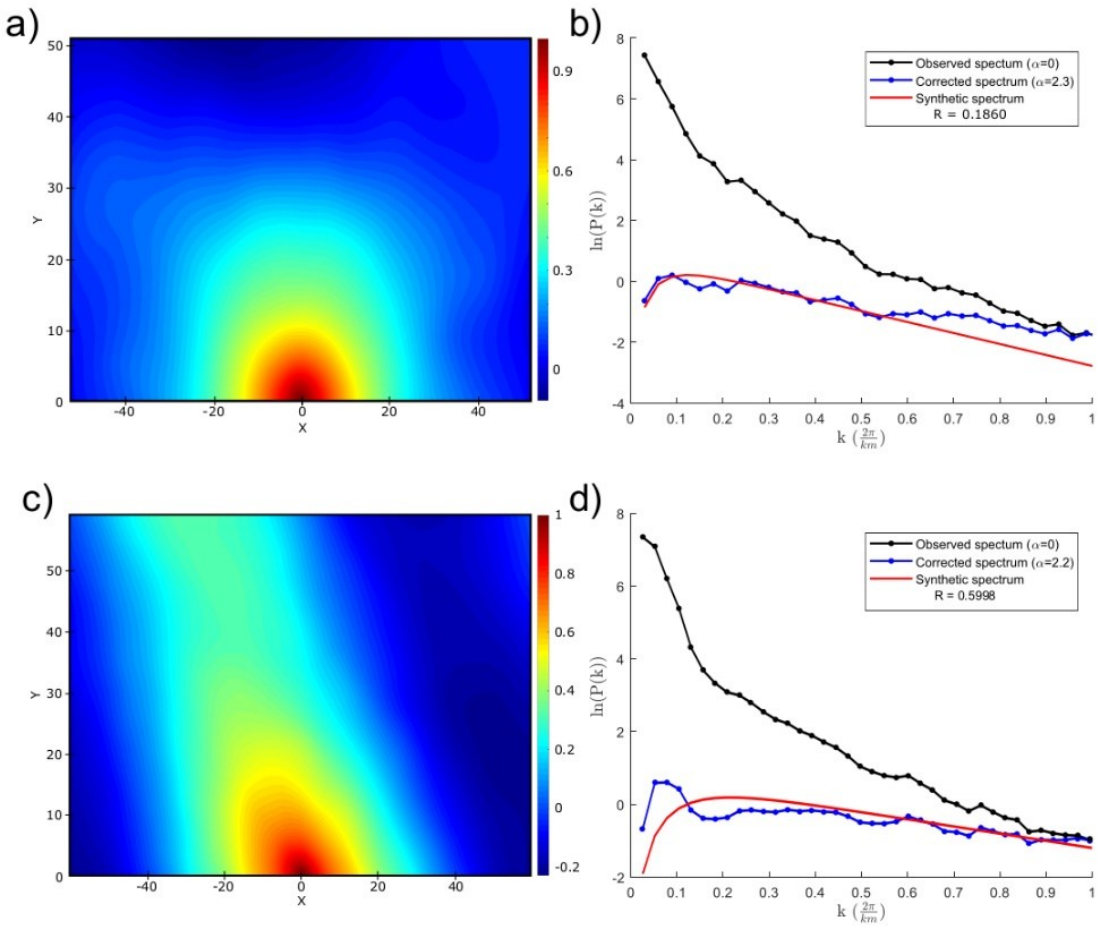

Figure 4: Spatial autocorrelation and spectra from windows VP1 (a, b) and 3-200 (c, d). For the near-circular autocorrelation, the modeled spectrum has low misfit values, while the ellipsoidal autocorrelation presents a large misfit value with the modeled spectra.

5. DISCUSSION

The window size is fundamental in DBMS calculation because a small window could not represent the deepest magnetic signal and the calculation is more likely related with shallower magnetic bodies, as in the case of window 7, where the calculation of DBMS is more realistic in the 250 x 250 km window than the 100 x 100 km window.

The strong trends are easily identified using the autocorrelation function. When it is not near-circular, the calculations may not be realistic. Analyzing carefully the spectra, we found high misfit values for the synthetic and the corrected spectrum, that is, the calculations are inconsistent. The trends observed in the autocorrelation function are very likely related with the Baja California batholith that has a strong trend for all the Baja California Peninsula.

The geological terrain is a key factor when selecting the window center, this is because a mixed signal has similar behavior to the case of a strong trend in the data that could affect the DBMS calculation and the autocorrelation function. In the case of the window VB of 210 x 210 km and 120 x 120 km, it was difficult to calculate the DBMS because it is not possible to adjust the synthetic spectrum. For VP1 and VP2 windows, the spectrum and the autocorrelation function present circularity, despite the complexity of the basement. This can be explained because the large window size analyzed allows detecting the deepest magnetic signal associated with the igneous and metamorphic basement that was found when drilling oil and gas wells.

Table 1: Depth to the bottom of magnetic source results.

Window number	Size (km)	α	Z_b (km)	Z_b uncertainty	R	Observations
1	120 x 120	1.9	21.0	0.55	0.2189	Visual inspection of spectral peak is not completely satisfactory and could not be adjusted further.
	200 x 200	1.8	34.5	2.20	0.4291	Spectral peak cannot be adjusted and there are gaps in magnetic data.
2	120 x 120	2.3	14.2	2.11	0.2746	Near-circular autocorrelation and good fit.
	200 x 200	2.2	21.8	2.28	0.2622	Near-circular autocorrelation and good fit.
3	120 x 120	2.5	17.7	0.96	0.2094	Good fit but autocorrelation function is not completely circular.
	200 x 200	2.2	12.9	1.98	0.5998	Spectral peak not fitted and non-circular autocorrelation function.
4	100 x 100	2.4	8.1	1.57	0.2861	Good autocorrelation but visual inspection of spectral peak is not completely satisfactory.
5	100 x 100	1.8	8.3	0.04	0.0907	Near-circular autocorrelation and good fit.
6	100 x 100	0	18.6	0.78	0.3603	Random and uncorrelated magnetization.
7	100 x 100	1.5	9.9	1.09	0.2164	Window size is not large enough.
	250 x 250	1.5	18.5	2.66	0.1577	Near-circular autocorrelation and good fit.
8	150 x 150	1.5	19.7	0.33	0.1325	Near-circular autocorrelation and good fit.
	250 x 250	1.5	24.3	2.99	0.1224	Near-circular autocorrelation and good fit.
VA	120 x 120	2.5	19.9	2.88	0.2625	Gaps in the magnetic data and not circular autocorrelation function.
	210 x 210	2.1	32.2	2.10	0.3524	Gaps in the magnetic data, not circular autocorrelation function and spectral peak not completely fitted.
VB	120 x 120	1.1	22.0	2.18	0.3402	Spectral peak not fitted and trend in autocorrelation function.
	210 x 210	1.3	17.1	1.74	0.2437	Window is on two tectonostratigraphic terranes, horizontal corrected spectrum and flat trend in autocorrelation function.
VP1	180 x 180	2.3	22.1	0.41	0.1860	Near-circular autocorrelation and good fit.
VP2	180 x 180	2.3	18.3	1.69	0.1247	Near-circular autocorrelation and good fit.

6. CONCLUSIONS

Ravat et al. (2007) suggestions on the processing of the aeromagnetic data and use the fractal corrections lead to obtaining realistic calculations. However, problems during the extraction of the IGRF or the strong trends observed in the autocorrelation function will deform the real slopes and produce erroneous results. The lack of data inside the windows is a frequent problem when calculating the DBMS. It is common that errors in the spectral analysis result from unsuitable window size or when the window includes highly different geological terrains. In those cases, the corrected spectrum fit is not attained and in most cases high values of misfit are derived; that is, results are not reliable and should not be used as representative of the DBMS.

The windows located on the borders of geological terrains of provinces probably will carry difficulties when calculating the DBMS. For this reason, it is suggested to keep the windows in geologically homogeneous areas. Some cases that will yield reliable results when the window includes diverse terrains is when their autocorrelation function is near-circular and there is good fit between spectra. In those cases, the spectrum is representative of the deepest magnetic source in the window.

REFERENCES

Bhattacharyya, B. K. and Lei-Kuang, Leu: Analysis of magnetic anomalies over Yellowstone National Park: Mapping of Curie point isothermal surface for geothermal reconnaissance. Journal of Geophysical Research, **80 (32)**, (1975), 4461-4465. doi: 10.1029/JB080i032p04461.

Blakely, R.J.: Curie temperature Isotherm Analysis and Tectonic Implications of Aeromagnetic Data from Nevada, Journal of Geophysical Research Solid Earth, **93(B10),** (1988), 11817-11832. doi: 10.1029/JB093iB10p11817

Blakely, R. J.: Potential Theory in Gravity and Magnetic Applications, Cambridge University Press, Cambridge (1995).

Bouligand, C., Glen, J. M. G. and Blakely, R. J.: Mapping Curie temperature depth in the western United States with a fractal model for crustal magnetization, Journal of Geophysical Research, **114**, (2009), B11104, doi:10.1029/2009JB006494.

Conrad, G., Couch, R. and Gemperle, M.: Analysis of aeromagnetic measurements from the Cascade Range in central Oregon, Geophysics, **48(3)**, (1983), 376-390. doi: 10.1190/1.1441476

Campos-Enriquez, J. O., Arroyo-Esquivel, M. A. and Urrutia-Fucugachi, J.: Basement, Curie isotherm and shallow-crustal structure of the Trans-Mexican Volcanic Belt, from aeromagnetic data, Tectonophysics, **172**, (1980), 77-90.

Campos-Enriquez, J. O., Espinosa-Cardeña, J. M. and Oskum, E.: Subduction control on the curie isotherm around the Pacific-North America plate boundary in northwestern Mexico (Gulf of California). Preliminary results, Journal of Volcanology and Geothermal Research, **175**, (2019), 1-17. doi: 10.1016/j.jvolgeores.2019.03.005

Espinosa-Cardeña, J. M. and Campos-Enriquez, J. O.: Curie point depth from spectral analysis of aeromagnetic data from Cerro Prieto geothermal area, Baja California, México, Journal of Volcanology and Geothermal Research, **176 (4)**, (2008), 601-609. doi: 10.1016/j.jvolgeores.2008.04.014

Espinosa-Cardeña, J. M., Campos-Enriquez, J. O. and Unsworth, M.: Heat flow pattern at the Chicxulub impact crater, northern Yucatan, Mexico, Journal of Volcanology and Geothermal Research, **311**, (2016), 135-149. doi: 10.1016/j.jvolgeores.2015.12.013

Gasparini, P., Mantovani, M. S. N., Corrado, G., and Rapolla A.: Depth of Curie temperature in continental shields: A compositional boundary? Nature, **278**, (1979), 845-846.

Gao, G., Kang, G., Li, G. and Bai, C.: Crustal magnetic anomaly and Curie surface beneath Tarim Basin, China, and its adjacent area, Canadian Journal of Earth Sciences, **52 (6)**, (2015), 357-367. doi: 10.1139/cjes-2014-0204

Haggerty, S. E.: Mineralogical constraints on Curie isotherms in deep crustal magnetic anomalies, Geophysical Research Letters, **5 (2)**, (1978), 105-108. doi: 10.1029/GL005i002p00105

Hsieg, H.-H., Chen, C.-H., Lin, P.-Y. and Yen, H.-Y.: Curie point depth from spectral analysis of magnetic data in Taiwan, Journal of Asian Earth Sciences, **90**, (2014), 26-33. doi: 10.1016/j.jseaes.2014.04.007

Li, C.-F., Shi X., Zhou, Z., Li, J., Geng, J. and Chen, B.: Depths to magnetic layer bottom in the South China Sea area and their tectonics implications, Geophysical Journal International, **182**, (2010), 1229-1247.

Li, C.-F, Lu, Yu and Wang, J.: A global reference model of Curie-point depths based on EMAG2, Scientific Reports, **7**, (2017), Article number: 45129. doi: 10.1038/srep45129

Manea, M. and Manea, V. C.: Curie Point Depth Estimates and Correlation with Subduction in Mexico, Pure and Applied Geophysics, **168 (8-9)**, (2011), 1489-1499. doi: 10.1007/s00024-010-0238-2

Martos, Y. M., Catalán, M., Jordan, T. A., Golynsky, A., Golynsky, D., Eagles, G. and Vaughan, D.G.: Heat Flux Distribution of Antarctica Unveiled, Geophysical Research Letters, **44 (22)**, (2017), 11,417-11,426. doi: 10.1002/2017GL075609

Martos, Y. M., Jordan, T. A., Catalán, M., Jordan, T. M., Bamber, J. L., and Vaughan, D. G.: Geothermal heat flux reveals the Iceland hotspot track underneath Greenland, Geophysical Research Letters, **45**, (2018), 1-9. doi: 10.1029/2018GL078289

Maus, S. and Dimri, V.: Potential field power spectrum inversion for scaling geology, J. geophys. Res., **100**, (1995), 12 605–12 616.

North America Magnetic Anomaly Group (NAMAG): Magnetic Anomaly Map of North America, US Geological Survey, (2002), 1-31.

Okubo, Y., Graf, R.J., Hansen, R.O., Ogawa, K. and Tsu H.: Curie point depths of the island of Kyushu and surrounding areas, Japan, Geophysics, **50**, (1985), 481-494.

Okubo, Y. and Matsunaga, T: Curie point depth in northeast Japan and its correlation with regional thermal structure and seismicity, Journal of Geophysical Research: Solid Earth, **99 (B11)**, (1995), 22 363-22 371.

Pilkington, M. and Todoeschuck, J.P.: Fractal magnetization of continental crust, Geophys. Res. Lett., **20**, (1993), 627–630.

Ravat, D., Pignatelli, A., Nicolosi, I. and Champpini, M.: A study of spectral methods of estimating the depth to the bottom of magnetic sources from near-surface magnetic anomaly data, Geophysical Journal International, **169 (2)**, (2007), 421-434. doi: 10.1111/j.1365-246X.2007.03305.x

Shuey, R. T., Schellinger, D. K., Tripp, A. C. and Al, L. B.: Curie depth determination from aeromagnetic spectra, Geophysical Journal of the Royal Astronomical Society, **50**, (1977), 75-101.

Rosales-Rodríguez, J., Bandy, W. L. and Centeno-García, E.: Profundidad de la base de la fuente magnética y estructura térmica del Golfo de México, Revista Mexicana de Ciencias Geológicas, **31 (2)**, (2014), 190-202.

Ross, H E., Blakely, R. J. and Zoback, M. D.: Testing the use of aeromagnetic data for the determination of Curie depth in California, Geophysics, **71 (5)**, (2006), L51-L59. doi: 10.1190/1.2335572

Salem, A., Green, C., Ravat, D., Singh, K. H., East, P., Fairhead, J. D., Mogren, S., and Biegert, E.: Depth to Curie temperature across the central Red Sea from magnetic data using the de-fractal method, Tectonophysics, **624–625**, (2014), 75–86, doi: 10.1016/j.tecto.2014.04.027

Spector, A. and Grant, F. S.: Statistical models for interpreting aeromagnetic data, Geophysics, **35 (2)**, (1970), 293-302. doi: 10.1190/1.1440092

Tanaka, A., Okubo, Y and Matsubayashi, O.: Curie point depth based on spectrum analysis of the magnetic anomaly data in East and Southeast Asia, Tectonophysics, **306 (3-4)**, (1999), 461-470. doi: 10.1016/S0040-1951(99)00072-4

Tsokas, G., Hansen, R. and Fytikas, M.: Curie Point Depth of the Island of Crete (Greece), Pure and Applied Geophysics, **152 (4)**, (1998), 747-757. doi: 10.1007/s000240050175

Wasilewski, P. J. and Mayhew, M. A.: The moho as a magnetic boundary revisited, Geophysical Research Letters, **19 (22)**, (1992), 2259-2262. doi: 10.1029/92GL01997

ACKNOWLEDGMENT

Aeromagnetic data was provided by the CeMIE-Geo. This work was funded by the -P01-CeMIE-Geo project "Geothermal Gradient and Heat Flow Maps of the Mexican Republic". To Pablo Velázquez-Sánchez and Katya Esquivel-Herrera, the summer internship students that helped with the spectral analysis and thanks to Gerald Gabriel for the Matlab code, this code was the base for the developing of de-fractal code.